0013-7227/08/$15.00/0
Printed in U.S.A.

Endocrinology 149(6):3137–3147

doi: 10.1210/en.2007-1525

Identification of an Upstream Promoter of the Human Somatostatin Receptor, hSSTR2, Which Is Controlled by Epigenetic Modifications

Jérôme Torrisani, Naïma Hanoun, Henrik Laurell, Frédéric Lopez, Jean-José Maoret, Anny Souque, Christiane Susini, Pierre Cordelier, and Louis Buscail

Institut National de la Santé et de la Recherche Médicale Unité 858-I2MR (J.T., N.H., H.L., A.S., C.S., P.C., L.B.), Institut de Médecine Moléculaire de Rangueil, Département Cancers Epithéliaux, Angiogénèse, et Signalisation, 31432 Toulouse Cedex 4, France; Institut Fédératif de Recherche 31 (F.L., J.-J.M.), Toulouse Rangueil, Plateformes de Génomique et Biologie Moléculaire/Protéomique et Intéractions Moléculaires, and Service de Gastroentérologie (L.B.), Centre Hospitalier Universitaire Rangueil, 31059 Toulouse, France

Somatostatin is a neuropeptide that inhibits exocrine and endocrine secretions of several hormones and negatively regulates cell proliferation. These events are mediated through somatostatin engagement on one of five G protein-coupled receptors named SSTR1 to STTR5. Somatostatin binding to SSTR2 mediates predominantly antisecretory and antiproliferative effects; two important biological activities in the gastroenteropancreatic endocrine and exocrine system. Herein we demonstrate novel regulatory sequences for human (h) SSTR2 transcription. By genomic DNA sequence analysis, we reveal two CpG islands located 3.8 kb upstream from the transcription start site. We identify a novel transcription start site and a promoter region within one of these CpG islands. We demonstrate that two epigenetic modifications, DNA methylation and histone acetylation, regulate the activation of hSSTR2 upstream promoter. Furthermore, we show that the transcription from this upstream promoter region directly correlates to hSSTR2 mRNA expression in various human cell lines. A combined treatment of a demethylating agent, 5-aza-2-deoxycytidine and a histone deacetylase inhibitor, trichostatin A, leads to increased expression of hSSTR2 mRNA in cell lines in which the CpG island is methylated. The epigenetic regulation of this promoter region results in differential expression of hSSTR2 mRNA in human cell lines. This study reveals the existence of a novel upstream promoter for the hSSTR2 gene that is regulated by epigenetic modifications, suggesting for complex control of the hSSTR2 transcription. (*Endocrinology* 149: 3137–3147, 2008)

SOMATOSTATIN IS A widely distributed neuropeptide that negatively regulates a number of cellular processes, such as the gastroenteropancreatic exocrine and endocrine secretions (1) and also exerts several effects in the central neuronal system (2). To date many studies have shown that somatostatin and its stable analogs suppress the growth of various normal and cancer cells (3). For example, somatostatin stable analogs (*i.e.* octreotide, lanreotide) are used for the treatment of endocrine tumors (4). There is also evidence for a direct antiproliferative effect mediated by specific cell surface receptors. Five G protein-coupled somatostatin receptors (SSTRs) subtypes termed SSTR1 to SSTR5 have been cloned from human and rodent (5), confirming that somatostatin exerts its various effects through binding to one of its cognate SSTRs. Among them, subtypes SSTR1, SSTR2, and SSTR5 are responsible for the antiproliferative effect of somatostatin and its analogs *in vitro* and *in vivo* (6, 7). In addition to antiproliferative properties, the human (h) SSTR2 can trigger apoptosis in NIH-3T3 cells (8). hSSTR2 is primarily expressed in normal brain, breast, pancreas, and kidney in humans (9). hSSTR2 is also robustly expressed in neuroendocrine tumors, yet its expression is dramatically reduced in human pancreatic exocrine adenocarcinomas and most of pancreatic cancer-derived cell lines (10–12). These observations draw a parallel with the immunohistochemistry and *in vivo* scintigraphy of human pancreatic exocrine adenocarcinomas, which show an absence of somatostatin-binding sites (13).

Although a number of studies have described somatostatin receptor hSSTR2 functions, few have investigated the transcriptional regulation of this gene. Previous findings identified transcription initiation start sites in a region located between 82 and 93 nucleotides upstream from the ATG translation start codon (9, 14–16). In close proximity to these initiation transcription sites, Pscherer *et al.* (15) described a initiation element (SSTR2 *inr*) that confers gene expression in the absence of a TATA-box. Glucocorticoid treatment *in vitro* leads to a significant inhibition of the hSSTR2 promoter, as mediated by two glucocorticoid-responsive elements (14). In contrast, 17β-estradiol, through an estradiol-responsive element located 3.8 kb from the transcription start site, was shown to activate hSSTR2 promoter activity (14, 16). Further analysis of the rodent SSTR2 gene demonstrated the existence of two spliced variants, SSTR2A and SSTR2B, located in the 3′ coding region of the gene (17). Other

First Published Online March 6, 2008

Abbreviations: 5-aza-dC, 5-Aza-2-deoxycytidine; ChIP, chromatin immunoprecipitation assay; FCS, fetal calf serum; GAPDH, glyceraldehyde-3-phosphate dehydrogenase; h, human; HDAC, histone deacetylase; HFH, hepatocyte nuclear factor; q-RT-PCR, quantitative real-time PCR; RACE, rapid amplification of cDNA ends; RT, reverse transcription; Sp, specificity protein; SSTR, somatostatin receptor; TSA, trichostatin A; UTR, unstranslated region.

***Endocrinology* is published monthly by The Endocrine Society (http://www.endo-society.org), the foremost professional society serving the endocrine community.**

studies demonstrated the existence of an upstream promoter of hSSTR5 and the murine SSTR2. Whereas these findings suggested the existence of additional upstream transcription start sites that control the hSSTR2 gene, these have yet to be determined (18, 19).

DNA methylation is the major DNA modification of the eukaryote genome that works to repress gene expression by rendering promoter regions silent. This modification occurs predominantly at position 5 of cytosines when followed by guanosines (dinucleotide CpG) (20). The reaction of methylation is catalyzed by a family of enzymes, known as DNA methyltransferases (21). With 85% of all CpGs methylated, only a minor part of the genome remains nonmethylated. Many of these nonmethylated CpGs are found in CpG islands (22). CpG islands are GC-rich regions of DNA, spanning an average of 1 kb. Interestingly, CpG islands coincide with the promoter region of approximately 60% of human RNA polymerase II-transcribed genes. Methylation of CpG islands and subsequent silencing of associated transcription units are found in genes located on the inactive X chromosome (23), genes silenced by genomic imprinting (24), and genes silenced in transformed cell lines and tumors (25). After DNA methylation, genes are silenced through the binding of methylated DNA-binding proteins that subsequently recruit repressive complexes such as histone deacetylases (HDACs) (26). Histone deacetylation, induced by HDACs in the vicinity of promoter regions, leads to a chromatin compaction that in turn provokes a transcriptional repression of the gene. Moreover, the binding on DNA of certain transcription factors, such as specificity protein (Sp1)-1, can be impaired by DNA methylation (27, 28).

In this study, we identify a novel promoter for the hSSTR2 gene located approximately 4.2 kb upstream from the previously characterized promoter. This region is within two CpG islands. We show that the transcription factor Sp1 is essential to the basal activity of this promoter. More interestingly, we demonstrate that the activity of this promoter is controlled by epigenetic modifications, including DNA methylation and histone acetylation. We further demonstrate that the epigenetic regulation of this promoter region results in differential expression of hSSTR2 mRNA in human cell lines.

Materials and Methods

Reagents

5-aza-dC and TSA were purchased from Sigma (Saint Quentin Fallavier, France).

CpG island determination

A 10.9-kb sequence contained in the *Homo sapiens* chromosome 17 genomic contig (GenBank no. NT_010641) from the position 5083977 to 5094877 was subject to the CpG plot software analysis (http://bioweb.pasteur.fr). For more straightforward readings, we designated the region 5083977 to 5094877 of GenBank contig NT_010641 as region −7662 to +3238, relative to the hSSTR2 transcription start site previously described (14). The parameters used to report a CpG island were set as follows: window size, 100 bp; minimum length for an island, 200 bp; window shift increment, 1; minimum observed to expected ratio, 0.6; and minimum percentage, 50. The percentage of GC within the 5′-UTR sequence was calculated using GeeCee software (http://bioweb.pasteur.fr/seqanal/interfaces/geecee.html).

Cell culture, treatment, and transfection

Human breast cancer MCF-7 and keratinocyte HACAT cells were both grown in DMEM medium (glucose 1 g/liter; Invitrogen, Cergy-Pontoise, France) supplemented with 10% fetal calf serum (FCS; Life Technologies, Inc.-BRL, Cergy-Pontoise, France), L-glutamine, antibiotics, and antifungics (Invitrogen). Human retinoblastoma cancer Y79 (ATCC HTB-18) and human exocrine pancreatic cancer Capan-1 cells (origin: liver metastasis) were grown in RPMI 1640 medium (Life Technologies, Inc.-BRL) whereas BxPC-3 (origin: primary tumor), PANC-1 (origin: primary tumor), and AsPC-1 cells (origin: ascite) were grown in DMEM (glucose 4.5 g/liter) supplemented with 10% FCS. Human pancreatic neuroendocrine tumor BON cells were grown in DMEM/HAM F12 (50%–50%) medium supplemented with 10% FCS. Human hepatoma HepG2 cells were grown in DMEM (glucose 4.5 g/liter) with 10% FCS. Human dermal microvascular endothelial HMEC cells were grown in MCBD 131 (Life Technologies, Inc.-BRL) supplemented with 10% FCS. Melanoma A7 cells (ATCC CRL-2500) were grown in MEM medium (Life Technologies, Inc.-BRL). Transfection of Y79, BON, PANC-1, and Capan-1 cells was performed using Fugene-6 (Roche Diagnostics, Meylan, France) following the manufacturer's recommendations. MCF-7 cells were transiently transfected using Exgen 500/PEI reagent (PolyPlus Transfection, Illkirch, France) following the manufacturer's recommendations.

Construction of luciferase reporter vectors containing different deletions of hSSTR2 upstream and downstream promoters

A pBluescript II hsst2p plasmid including a 7.0-kb fragment that includes the coding region of hSSTR2 and 5.5 kb of the 5′-flanking sequence was a generous gift from Dr. J. F. Bruno (Stony Brook University, Stony Brook, NY). The 5.5-kb fragment corresponding to the 5′-flanking region was deleted from the pBluescript II hsst2p plasmid and inserted into pGL_3 Basic vector (Promega, Charbonnières-les-Bains, France) between *Xho*I and *Nco*I restriction sites (5500–5′ flanking region-LUC) [position −5375 to +95, relative to the transcription start site described in (14)].

Deletion constructs of hSSTR2 upstream promoter: a *Kpn*I and *Nhe*I fragment was released from 5500–5′ flanking region-LUC vector and inserted into pGL_3 basic vector to generate 1200-upstream-LUC construct (−1152 to +107, relative to the upstream transcription start site). A 230-bp *Sma*I/*Nhe*I fragment (−123 to +107) was deleted from the 1200-upstream-LUC vector to produce ΔTSS-upstream-LUC construct. The Δ820–120-upstream-LUC plasmid was created by deleting a *Pst*I fragment (−822 to −118) from the 1200-upstream-LUC construct. Fragments *Kpn*I/*Pvu*II (−1152 to −330), *Kpn*I/*Pst*I (−1152 to −118) and *Kpn*I/*Apa*I (−1152 to −27) were deleted from the 1200-upstream-LUC plasmid to obtain 330-upstream-LUC (−330 to +107), 120-upstream-LUC (−118 to +107), and 30-upstream-LUC (−27 to +107) constructs, respectively.

For deletion constructs of the hSSTR2 downstream promoter, the construction of 4200-downstream-LUC [−4205, relative to the downstream transcription start site described elsewhere (14)], 3700-downstream-LUC (−3728 to +95), and 800-downstream-LUC (−825 to +95) plasmids was accomplished after deletion of the fragments generated by digestion of the 5500–5′ flanking region-LUC plasmid with enzymes *Nhe*I, *Kpn*I, and *Sac*I, respectively. The constructs 200-downstream-LUC (−202 to +95) and 40-downstream-LUC (−38 to +95) were generated by creating restriction sites on the 5500–5′ flanking region-LUC vector using the site-directed mutagenesis kit (Stratagene, Amsterdam, The Netherlands). The appropriate fragments were deleted and the vectors were religated.

The plasmids pCMV-Sp1, -Sp3, and -Sp4 were provided by Dr. S. Shaak (Institut National de la Santé et de la Recherche Médicale Unité 858, Toulouse, France).

5′-RACE analysis

The 5′-RACE was performed on 5 μg of Y79 cell total RNA using the 5′-RACE system for rapid amplification of cDNA ends, version 2.0 (Invitrogen) following the manufacturer's recommendations. The gene-specific primer sequence used to obtain the 5′-RACE products was

5′-AAAGGCAGACCCAGCATGAA-3′. Primers used for PCR amplification were abridged universal amplification primer provided by the kit and 5′-TATTGGTTGACACCACAGAGCC-3′ located on the coding sequence and 159 nucleotides from the previously identified transcription start site (14). PCRs were performed at an annealing temperature of 60 C. 5′-RACE products were analyzed by PAGE followed by ethidium bromide staining and fragments were cloned into pCR2.1 TOPO vector (Invitrogen). After bacterial transformation, individual colonies were grown, and plasmid DNA was purified and subject to sequencing using M13 universal primers.

Luciferase activity

Transfections of Y79, BON, MCF-7, PANC-1, and Capan-1 cells were performed in triplicate. One microgram of luciferase reporter plasmids per 35-mm dish was transfected. Luciferase activity was measured using the luciferase assay system (Promega) following the manufacturer's protocol. Variability in transfection efficiencies was normalized by cotransfection with a β-galactosidase-expressing vector pSV-β-Gal (Promega). β-Galactosidase activity was measured using the β-galactosidase enzyme assay system (Promega). Experiments were performed in triplicate. Cotransfection experiments were performed using 1 μg/dish of pCMV-Sp1, -Sp3, and -Sp4 vectors or empty plasmid.

Sequence alignment and determination of putative transcription binding sites conserved across species

The 1216-nt genomic sequence flanking the upstream hSSTR2 transcription start site and 268 nucleotides corresponding to the exonic sequence (accession no. NT_010641) were compared with mouse and rat genomic sequence data bank (Blastn software, www.ncbi.nlm.nih.gov). High homologies were found with the mouse exon 2 and its upstream region (accession no. AJ005519 from nt 1 to 1341) as well as the rat exon 1 and its upstream region (accession no. AB047297 from nt 2957 to 4364). The three sequences were aligned using Multalin software (version 5.4.1) (29). Transcription factor binding sites conserved between species were identified using TFSEARCH software (http://www.cbrc.jp/research/db/tfsearch.html). TFSEARCH searches for highly correlated sequence fragments against the TFMATRIX, a transcription factor binding site profile database in the TRANSFAC databases by GBF-Braunschweig. The threshold score was set at 85%.

Chromatin immunoprecipitation assay (ChIP)

Kit ChIP assays were performed following the recommended protocol from the manufacturer (EZ ChIP ChIP kit; Upstate Biotechnology, Saint Quentin en Yvelines, France), using antiacetylated histone (Upstate 06-599), anti-Sp1 (sc-59; Santa Cruz Biotechnology Inc., Heidelberg, Germany) and rabbit IgG (Santa Cruz Biotechnology) antibodies. The amount of hSSTR2 upstream region was quantified by quantitative RT-PCR using two sets of primers: hSSTR2 ChIP A, forward 5′-TCCCCCGGCTGTCTGTA-3′ and reverse 5′-GGGTGAGACCGGCTGAAAC-3′; hSSTR2 ChIP B, forward 5′-AGCCCCAGTATG AGGATTGG-3′ and reverse 5-GCTAGCCCCTCGCACGTA-3′. The positions of the primers are represented in Fig. 4A. The relative binding of specific antibody to the target sequence was determined by comparing the calculated amount of precipitated DNA with the amount of that sequence in the input DNA.

q-RT-PCR

Total RNAs were isolated using Trizol reagent (Invitrogen) in accordance with the manufacturer's protocol. To quantify the amount of RNA and verify quality, all samples were analyzed by Agilent Technology (Massy, France). Five micrograms of total RNA were reverse transcribed using Superscript III (Invitrogen) and random primers in a 50 μl final volume.

Primers for q-RT-PCR were designed using Primer Express software (PE Applied Biosystems, Warrington, UK). The sequences are the following: hSSTR2 upstream forward, 5′-GTGTCGGAGACCGGAGCTAG-3′ and reverse, 5′-GGAGGCCAAGGATCCAGTG-3′; hSSTR2 total forward, 5′-TTTTGTGGTCTGCATCATTGG-3′ and reverse, 5′-AAAGGCAGACCC AGCATGAA-3′;18S rRNA forward, 5′-AAACGGCTACCACATCCAAG-3′ and reverse, 5′-CCT CCAATGGATCCTCGTTA-3′ (30); β-actin forward, 5′-AGATGTGGATCAGCAAGCAGGAGT-3′ and reverse, 5′-GCAATCAAAGTCCTCGGCCACATT-3′ (31); glyceraldehyde-3-phosphate dehydrogenase (GAPDH) forward, 5′-CAATGACCCCTTCATTGACC-3′ and reverse, 5′-GATCTCGCTCCTGGAAGATG-3′. Serial dilutions of a hSSTR2 containing plasmid (1 $\mu g/\mu l$) ranging from 10^{-6} down to 10^{-9} were used as templates to compare the efficiency of hSSTR2 exon *vs.* hSSTR2 open reading frame primer sets. PCR amplifications were performed using the ABI-7900 apparatus (PE Applied Biosystems) using SYBR green technology (SYBR Green PCR master mix, PE Applied Biosystems). Dissociation curve and analysis using agarose gel electrophoresis were performed to ensure the amplification of a single PCR product to compare the level of hSSTR2 mRNA between the different cell lines. Although the level of ribosomal RNAs that constitute up to 80% of the total RNAs is thought not to vary under conditions that affect the expression of mRNAs, we decided to add two other normalization control cDNA: GAPDH and β-actin. Each sample was quantified in duplicate and negative controls were performed according to standard protocols.

In vitro methylation assay

The 1200-upstream-LUC and pGL_3 basic control plasmids were *in vitro* methylated by incubation with *Sss*I CpG methylase (New England Biolabs, Saint Quentin-en-Yvelines, France) in the recommended buffer. Complete methylation was verified by digestion with the methylation-sensitive *Hpa*II enzyme. Methylated plasmid was recovered by phenol/chloroform extraction and ethanol precipitation. As control, both plasmids were subject to the same treatment in the absence of *Sss*I methylase. Plasmids were transfected and after 24 h, luciferase activity was measured as described above.

Bisulfite mapping analysis

Genomic DNA was extracted using a genomic DNA extraction kit (Promega). Five to 10 micrograms were subject to sodium bisulfite treatment. Briefly, genomic DNA was digested with *Eco*RI (MBI-Fermentas, Mundolsheim, France) and purified using PCR purification kit (QIAGEN, Courtaboeuf, France). DNA was then denatured in NaOH (0.3 M) for 15 min at 37 C. Cytosines were sulfonated in sodium bisulfite (3.6 M; Sigma) and hydroquinone (1 mM; Sigma) overnight at 55 C in a thermocycler. The DNA samples were desalted through a column (Methylamp DNA modification kit; Epigentek Inc., Mundolsheim, France). DNA concentrations were determined by ND-1000 technology (NanoDrop, Wilmington, DE).

Primers for bisulfite mapping were designed by Methyl Primer Express Software (version 1.0; Applied Biosystems): hSSTR2 BS forward, 5′-GGTTGGTTGGGTTAGTTTTAG-3′ and reverse 5′-TTTA AAATTCCTAACTCCTCAAC-3′; they amplify a 179-bp DNA fragment corresponding to the region between the positions −25 to +154, relative to the upstream transcription start site containing 16 CpG dinucleotides. PCR amplification was performed from 10 to 20 ng of modified DNA in a 50-μl reaction containing 1× buffer, 0.2 pmol of each primer, 1.5 mM $MgCl_2$, 0.2 nmol deoxynucleotide triphosphates, 1.25 μl Ampli Taq Gold (5 $U/\mu l$) polymerase (PE Applied Biosystems). First denaturation step was 10 min at 95 C, 40 cycles of denaturation at 95 C for 15 sec, and annealing at 55 C for 30 sec, and extension at 72 C for 15 sec followed and final extension at 72 C for 7 min. PCR products were visualized by PAGE followed by ethidium bromide staining and cloned into pCR2.1 vector (Invitrogen). Colonies were grown and plasmidic DNA was extracted using NucleoSpin plasmid kit (Macherey-Nagel, Hoerdt, France) and digested with *Eco*RI restriction enzyme. Positive clones, containing a 179-bp PCR fragment, were sequenced on both strands using automatic sequencer (Millegen, Labège, France).

Statistical analysis

Experiments were performed in triplicate. Averages and SDs were calculated. Student's *t* test and Spearman ρ-test were performed using the Biostatgv Web site (www.u707.jussieu.fr/biostatgv), and critical value for statistical significance ($P < 0.05$) is indicated.

Results

Identification of two CpG islands located 3.8 kb upstream from the transcription start site

Previous studies have reported transcription start sites for the hSSTR2 gene. They characterized a promoter region containing an initiator element located at the proximity of the ATG translation start site (Fig. 1) that generated an 82-to-93 nucleotide-unstranslated region (5′-UTR) (9, 15, 16). Recent findings of an upstream promoter for the human SSTR5 and murine SSTR2 led us to investigate whether the hSSTR2 gene contained an upstream promoter element that could be silenced by DNA methylation. It was possible that an upstream promoter evaded discovery due to a silencing by DNA methylation. We first submitted the genomic DNA sequence of hSSTR2 gene to bioinformatic analysis to predict and localize CpG islands. The commonly accepted criteria that define a CpG island were set as follows: minimum length 200 bp, GC content greater than 50% and ratio CpG observed/expected greater than 0.6. A 10.9-kb sequence (GenBank contig NT_010641, nt 5083977 to 5094877) that contains the hSSTR2 coding region flanked by the UTRs (5′- and 3′-) as well as approximately 7.7 kb of the 5′-flanking region was analyzed. For more straightforward readings, we designated the region 5083977–5094877 of the GenBank contig as −7662 to +3238, relative to the hSSTR2 transcription start site described elsewhere (14). The analysis revealed the presence of two CpG islands spanning on approximately 1 kb located approximately 3.8 kb upstream from the transcription start site (Fig. 1, *bottom panel*). No other CpG islands were predicted in the submitted sequence. The presence of CpG islands led us to speculate for the existence of a putative promoter region located within this region.

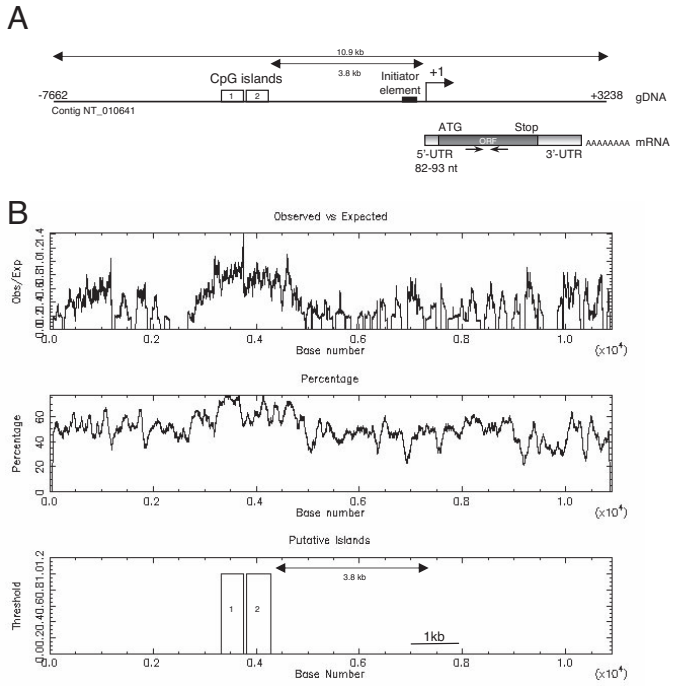

FIG. 1. Bioinformatic analysis of the 5′-flanking genomic DNA sequence upstream from hSSTR2 transcription start site. A, Graphical representation of 10.9 kb of the hSSTR2 genomic sequence (gDNA) is represented (GenBank accession no. NT_010641). The positions −7662 and +3238 are relative to the transcription start site (*arrow* and +1) described elsewhere (14). The initiator element previously described (15) is represented by a *filled box*. *Empty rectangles* numbered 1 and 2 represent the location of two CpG islands identified in B. hSSTR2 mRNA representation shows the 5′-UTR and 3′-UTR, the poly-A tail, and the open reading frame. The *arrows* in the opposite direction represent the primer set (hSSTR2 total) used for q-RT-PCR. B, Graphical representation of the CpG islands identified within the hSSTR2 gene. The *upper panel* represents the ratio of CpG observed to CpG expected, whereas the *middle panel* represents the GC content calculated as a percentage of total. The *bottom panel* represents the two CpG islands (numbered 1 and 2) within the 10.9-kb hSSTR2 sequence.

Relative abundance of total hSSTR2 mRNA in different human cell lines

DNA methylation can maintain promoters silent when located in a CpG island. To reveal the presence of an upstream hSSTR2 promoter that could be silenced by DNA methylation, we decided to select a human cell line that expresses a high level of hSSTR2 mRNA, suggesting that a putative upstream promoter would not be repressed. The relative abundance of hSSTR2 mRNA was measured by quantitative real-time PCR (q-RT-PCR). The position of the primers used for these analyses are represented in Fig. 1. Among 11 human cell lines from different origin, retinoblastoma Y79, pancreatic neuroendocrine cancer BON, hepatoma HepG2, breast cancer MCF-7, and melanoma A7 cells displayed the highest levels of hSSTR2 mRNA expression (Fig. 2). In contrast, we classified the remaining six cell lines as low hSSTR2 mRNA-expressing cell lines. These included the keratinocyte HACAT; mammary endothelial HMEC; and the pancreatic cancer PANC-1, Capan-1, BxPC-3, AsPC-1 cell lines.

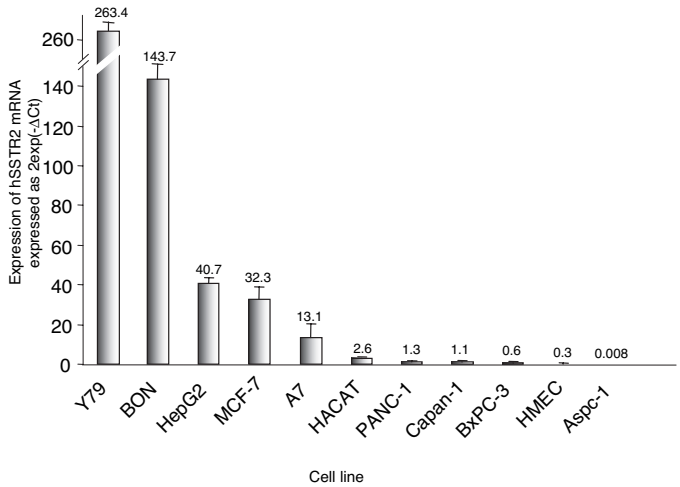

FIG. 2. Relative abundance of total hSSTR2 mRNA in different human cell lines. The amount of total hSSTR2 mRNA in the indicated cell lines was quantified by q-RT-PCR analysis. Primers located in hSSTR2 coding sequence (hSSTR2 total, Fig. 1A) were used. β-Actin, GAPDH, and 18S rRNA amplification were used for normalization. Represented results are expressed as 2exp(-ΔCt) using β-actin as the reference gene. Values are indicated *above the bars*. Experiments were performed in triplicate.

Identification of an upstream transcription start site

Due to a high expression level of hSSTR2 mRNA, we decided to pursue the identification of a putative upstream promoter in the retinoblastoma Y79 cells. Total RNAs from these cells were extracted and subjected to a 5′-rapid amplification of cDNA ends (RACE) analysis (see *Materials and Methods*). Three PCR products, with approximate sizes of 180, 270, and 300 bp, were observed (Fig. 3A). The three PCR bands were subsequently cloned and sequenced. Sequencing of the approximately 180-bp PCR fragment revealed a sequence corresponding to a region located immediately upstream from the ATG translation start site of hSSTR2 gene situated on chromosome 17. This result confirmed the presence of the transcription start site located 91 nucleotides from the ATG translation start site, which was previously described (Fig. 3B) (14–16). However, the sequencing of the approximately 300-bp PCR fragment revealed a sequence that corresponded to the 91 first nucleotides from the ATG codon but extended by 266 nucleotides. Sequence alignment showed that these 266 nucleotides corresponded to a sequence on chromosome 17 but were located at positions −3939 to −4205 upstream from the transcription start site described elsewhere (14). This result revealed the existence of an upstream transcription start site located approximately 4.2 kb upstream from the one previously described. Therefore, these findings confirmed our hypothesis for the existence of an upstream transcription site in one of the two CpG islands we identified (Figs. 1 and 2B).

The sequencing of the 270-bp PCR fragment revealed the same sequence as the 300-bp fragment but lacked 30 nucleotides at the 5′ extremity. This could suggest the presence of another initiation transcription start site located 30 nucleotides downstream from the newly identified upstream transcription start site. However, the 270-bp PCR fragment is most likely due to incomplete reverse transcription (RT) during the 5′-RACE experiment.

The analysis of the sequence junctions in the hSSTR2 genomic DNA revealed the presence of 5′-donor and 3′-acceptor splicing sequences. Indeed, the sequence at the 5′-side of the hSSTR2 mRNA junction 5′-AAG-gugag-3′ (position −3941 to −3948) showed a high homology with the consensus sequence 5′-(C/A)AG-gu(a/g)ag-3′ described by Ogbourne and Antalis (32) (Fig. 3C). In parallel, the sequence of the 3′-side of the junction cuuccucuuuuccuuccag-A (position +1 to −18) matched with the consensus sequence 5′-(u/c)11n(u/c)ag(G/A)-3′. These results demonstrated that hSSTR2 mRNA can be encoded by two exons separated by a 4.2-kb intronic sequence that must be removed by a splicing process. Although the hSSTR2 mRNA transcription starts from two distinct genomic regions that generate different 5′-UTRs, the sequence of the open reading frame does not change. In addition, transcription from the upstream promoter leads to a highly CG-rich 5′-UTR (66%) with a size of 357 bp, which might generate stable mRNA secondary structures.

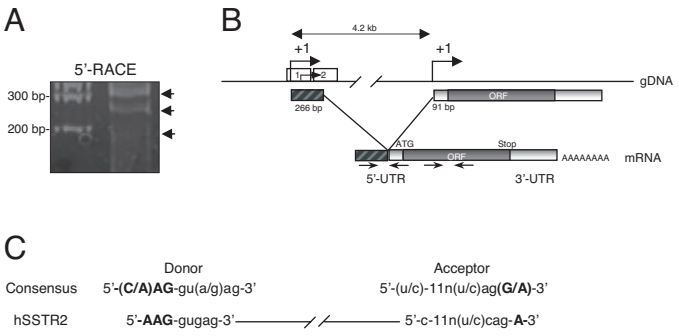

FIG. 3. Localization of the hSSTR2 upstream transcription start site by 5′-RACE analysis. A 5′-RACE PCR amplification was visualized by electrophoresis on agarose gel followed by ethidium bromide staining. Estimation of PCR product size (*right lane*) was determined by comparison with the Smart DNA ladder (*left lane*). B, Graphical representation of the location of hSSTR2 transcription start sites. The *arrows* +1 indicate the two transcription start sites separated by an approximately 4.2 kb genomic region. The *small arrow* represents a putative transcription start site. mRNA generated after RNA splicing is represented. *Empty rectangles* (1 and 2) indicate the location of the two CpG islands on the genomic sequence. The two pairs of *arrows* in opposite directions represent the position of the two sets of primers used in Fig. 5. C, hSSTR2 donor and acceptor splicing sites, compared with the donor and acceptor consensus sequences defined by Ogbourne and Antalis (29).

Determination of putative transcription binding sites on the hSSTR2 upstream promoter region that are conserved across species

An approximately 1.2-kb sequence located upstream from the new transcription start site and 268 nucleotides corresponding to the exonic sequence were compared with a mouse and rat genomic sequence data bank. The alignment revealed high homologies with genomic regions located upstream from the mouse SSTR2 exon 2 (accession no. AJ005519) and rat exon 1 (accession no. AB047297) (Fig. 4A). Interestingly, the new transcription start site is located close to a region in which the transcription start site of the rat exon 1 was previously determined (33) and near a region of the mouse exon 2 transcription start site (18). Similarly to the mouse and rat promoter, the human upstream promoter lacks TATA or CAAT box consensus sequences. Putative transcription factors binding sites in the highly conserved regions were determined using TFSEARCH software (http://www.cbrc.jp/research/db/tfsearch.html). A previous study showed the functional importance of both cAMP responsive element and Sp1 sites in regulating rat SSTR2 promoter activity (33). Whereas the Sp1 site (−47 to −55, relative to the upstream transcription start site) displays a high homology on the human promoter sequence, the cAMP responsive element site (−64 to −71) is not conserved in the human sequence. This suggests that the Sp1 transcription factor could contribute to basal promoter activity. Although other putative transcription factor-binding sites were identified in the rat and mouse promoter (glucocorticoid response element, estrogen response element, paired-like homeodomain transcription factor 1) (18, 33), these sites were not found highly conserved in the human sequence, suggesting a smaller role of these transcription factors in the control of the human upstream promoter. In contrast, several other putative transcription-binding sites were found highly conserved within a region located at position −721 to −861 (Fig. 4A). The Oct-1, hepatocyte nuclear factor (HFH)-1 and p300 proteins could potentially regulate the human upstream promoter. We also observed the presence in all three

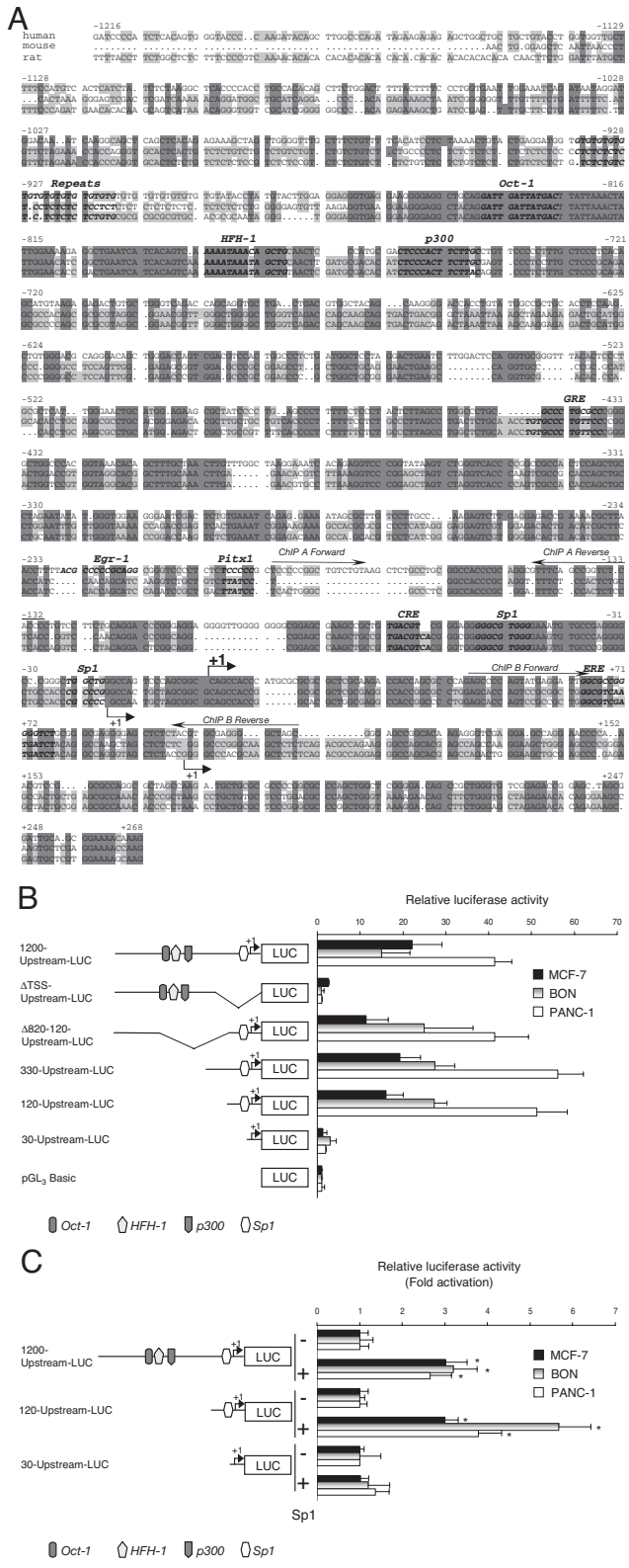

FIG. 4. Characterization of the hSSTR2 upstream promoter. A, Homologies between the human genomic sequence of hSSTR2 exon 1 flanked by a 1216-nt upstream region (accession no. NT_010641) and mouse or rat genomic sequence data banks were searched using Blastn software (www.ncbi.nlm.nih.gov). The alignment of the hSSTR2 sequence with the mouse exon 2 and the rat exon 1 sequences flanked by their upstream region (accession no. AJ005519 from nt 1 to 1341 and accession no. AB047297 from nt 2957 to 4364, respectively) was performed using Multalin software. Putative transcription binding sites were determined using TFSEARCH software, and only those conserved across species are shown in *bold* and *italic* font. The *arrow* / *+1* symbols above or below the nucleotides in *white* indicate the position of the SSTR2 transcription start sites in the three different species. The number of the nucleotides is relative to the human upstream transcription start site. Sequences that are conserved between two species are highlighted in *light gray*; sequences common to the three species are highlighted in *dark gray*. The two sets of *black thin arrows* indicate the position of the primers (*ChIP A* and *ChIP B*) used in the ChIP (Fig. 6, B and C). B, Different deletions of the hSSTR2 upstream promoter were inserted into a luciferase reporter pGL$_3$ basic vector. MCF-7, BON, and PANC-1 cells were transiently transfected and luciferase activity was measured after 24 h. To avoid variability due to transfection efficiency, vector encoding β-galactosidase was cotransfected, and β-galactosidase activity was measured on the same extracts. Transfection experiments (n = 3) were performed in triplicate. Positions of the putative binding sites for the transcription factors Oct-1, HFH-1, p300, and Sp1 are represented on the constructs. For ΔTSS-Upstream-LUC, TSS stands for transcription start site. C, Different hSSTR2 upstream promoter constructs were cotransfected with a Sp1 expressing (+) or an empty plasmid (−) into MCF-7, BON, and PANC-1 cells. Luciferase activity was measured 24 h later. Transfection experiments (n = 3) were performed in triplicate.

species of dinucleotide repeat sequences located from position −900 to −938.

Characterization of the hSSTR2 upstream promoter

To evaluate the potential of the hSSTR2 upstream region to initiate transcription and determine the transcription factor-binding sites that contribute to the basal promoter activity, we inserted different deletions of this region in a luciferase reporter plasmid (Fig. 4B). The reporter constructs were transiently transfected into MCF-7, BON, and PANC-1 cells. Measurements of luciferase activity revealed that an approximately 1.3-kb DNA fragment encompassing the upstream transcription start site (1200-Upstream-LUC) was capable of initiating transcription of the reporter gene (Fig. 4B). In parallel, we observed that the deletion of the region containing the transcription start site (ΔTSS-Upstream-LUC) led to a dramatic reduction of luciferase activity. This result confirmed the transcriptional activity of this new hSSTR2 upstream promoter. The deletion of a region containing the binding sites for the transcription factors Oct-1, HFH-1, and p300 (Δ820–120-Upstream-LUC) did not significantly affect the transcriptional activity. Reporter constructs containing approximately 330 or approximately 120 bp upstream from the transcription start site (330-Upstream-LUC and 120-Upstream-LUC, respectively) displayed a similar activity as the 1200-Upstream-LUC, suggesting the importance in the basal transcriptional activity of these remaining 120 nucleotides. The analysis in Fig. 4A revealed the presence in this region of a highly conserved Sp1 transcription factor binding site. Interestingly, the deletion of this putative binding site (30-Upstream-LUC) led to the total reduction of the transcriptional activity. This result demonstrated the contribution of this Sp1 binding site in the basal transcriptional activity of the upstream promoter. This finding is in agreement with number of studies showing that the ubiquitously expressed Sp1 transcription factor regulates numerous TATA-less and CAAT-less promoters in mammalian cells (27). In parallel,

serial deletions of the downstream promoter confirmed the role of the initiator element described by Pscherer *et al.* (15), which confers a minimal transcriptional activity to this promoter. However, it is important to notice the lower transcriptional activity of the downstream promoter, compared with the upstream promoter (supplementary data S1, published as supplemental data on The Endocrine Society's Journals Online Web site at http://endo.endojournals.org).

To ensure the role of the transcription factor Sp1 in the upstream promoter activity, cotransfection experiments were performed in MCF-7, BON, and PANC-1 cells (Fig. 4C). Whereas the transfection of a vector encoding Sp1 transcription factor enhances the activity of the 1200-Upstream-LUC and 120-Upstream-LUC constructs, the overexpression of Sp1 has no effects on either 30-Upstream-LUC or pGL_3 basic constructs. No effects on 1200-Upstream-LUC activity of an overexpression of transcription factors Sp3 or Sp4 could be observed (supplementary data S2). These data confirmed the contribution of the transcription factor Sp1 in the basal activity of the hSSTR2 upstream promoter.

Cell line-specific usage of the human hSSTR2 upstream promoter

Because we identified an upstream promoter region able to initiate the transcription of hSSTR2 mRNA, we decided to evaluate the participation of this promoter region on the total expression of hSSTR2 mRNA in different cell lines. We designed two set of primers for q-RT-PCR such that one amplified total hSSTR2 mRNA, whereas the other specifically amplified hSSTR2 mRNA produced by the upstream promoter (see *Materials and Methods* and Fig. 3B). Both set of primers showed the same amplification efficiency (supplementary data S3). We performed RT and q-RT-PCR on RNA extracted from different human cell lines (Fig. 5). In three of the nine cell types assayed (Y79, BON, and MCF-7), the upstream promoter was responsible of 40–60% of the total hSSTR2 mRNA expression. Interestingly, these cell lines also express a relatively high level of hSSTR2 mRNA, compared with the others (Fig. 2). In contrast, in the other six cell lines, the implication of the upstream promoter in hSSTR2 mRNA expression was weak. Among them, HMEC, Capan-1, BxPC-3, and HACAT express a very low level of hSSTR2 mRNA (Fig. 2). These data suggested that the use of the upstream promoter by a cell leads to a higher hSSTR2 mRNA expression level.

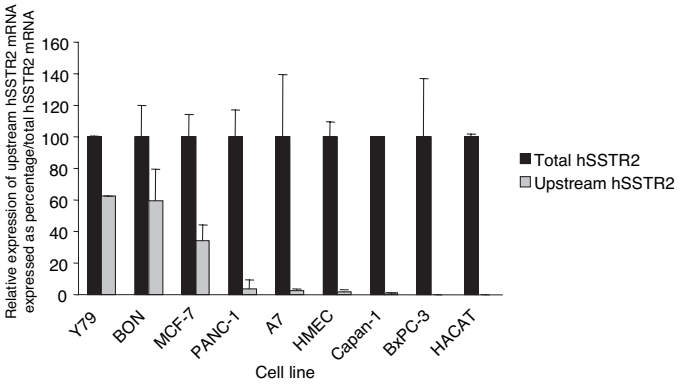

FIG. 5. Measurement of hSSTR2 mRNA transcribed from the upstream promoter in different human cell lines. The amount of hSSTR2 mRNA transcribed from the upstream promoter was measured by q-RT-PCR using a set of primers that amplify specifically hSSTR2 mRNA transcribed from this promoter. The mRNA level was compared with the total hSSTR2 mRNA level, which was represented as 100%. To compare both mRNA levels, both set of primers were chosen with the same amplification efficacy (supplementary data S3 and Fig. 3B). Results are represented as the percentage of hSSTR2 mRNA transcribed from the upstream promoter in comparison with the total amount of hSSTR2 mRNA (100%) in the cells. Experiments (n = 3) were performed in triplicate. β-Actin amplification was used to normalize values.

Methylation status of hSSTR2 CpG island in different human cancer cell lines is inversely correlated with hSSTR2 mRNA expression and Sp1 binding

The observation that the upstream hSSTR2 promoter is functional in some cell lines and inactive in others led us to investigate the reasons of this inactivation. DNA methylation leads to a chromatin compaction and the silencing of promoters located in the vicinity of or embedded in this methylated region. A 179-bp genomic region located within the CpG island 1, containing the hSSTR2 upstream transcription start site was analyzed by sodium bisulfite mapping (Fig. 6A). The percentage of methylated CpG in this region was calculated for 11 different cell lines. Interestingly, cell lines displayed different percentage of methylated CpG in the hSSTR2 CpG island 1. Whereas Y79, BON, or A7 cell lines showed no methylated CpG, the human pancreatic cancer AsPC-1 and Capan-1 cells as well as the human mammary endothelial HMEC cells presented a high percentage of methylated CpG (58, 58, and 64%, respectively). Other cell lines such as MCF-7 or BxPC-3 revealed a moderate percentage of methylated CpG (12.5 and 11.5%, respectively). DNA methylation and histone acetylation are tightly linked. Chromatin immunoprecipitation assays revealed a lower association of acetylated histones H3 with hSSTR2 upstream region when it is methylated (Fig. 6B).

Interestingly, we observed that a low percentage of methylated CpG in hSSTR2 upstream region (0, 0, 6, and 12.5%, respectively) correlates with a high level of hSSTR2 mRNA in the Y79, BON, HepG2, and MCF-7 cell lines (Fig. 2). Moreover, we noted that the upstream promoter is responsible of 40–60% of the total hSSTR2 mRNA expression in Y79, BON, and MCF-7 cells (Fig. 5). In contrast, cell lines that display high level of methylated CpG such as HMEC, AsPC-1, and Capan-1 (64, 58, and 58%, respectively) express hSSTR2 mRNA at a low level (Fig. 2). In addition, the participation of the upstream promoter in hSSTR2 mRNA expression in HMEC and Capan-1 cells is weak (Fig. 5). This inverse correlation observed between hSSTR2 CpG island methylation and hSSTR2 mRNA expression is statistically supported by a Spearman ρ-test ($P < 0.05$). Furthermore, previous studies reported that the binding of the transcription factor Sp1 is inhibited by DNA methylation of adjacent CpG sites of its target sequence (28). We demonstrated that Sp1 contributes to the basal transcription activity of the upstream hSSTR2 promoter (Fig. 4, B and C). In Fig. 6C, we showed a lower association of Sp1 with the hSSTR2 upstream region when it is highly methylated (HMEC and Capan-1 cells) in comparison with a nonmethylated upstream region (Y79 and BON cells).

Taken together, these results demonstrated that a high

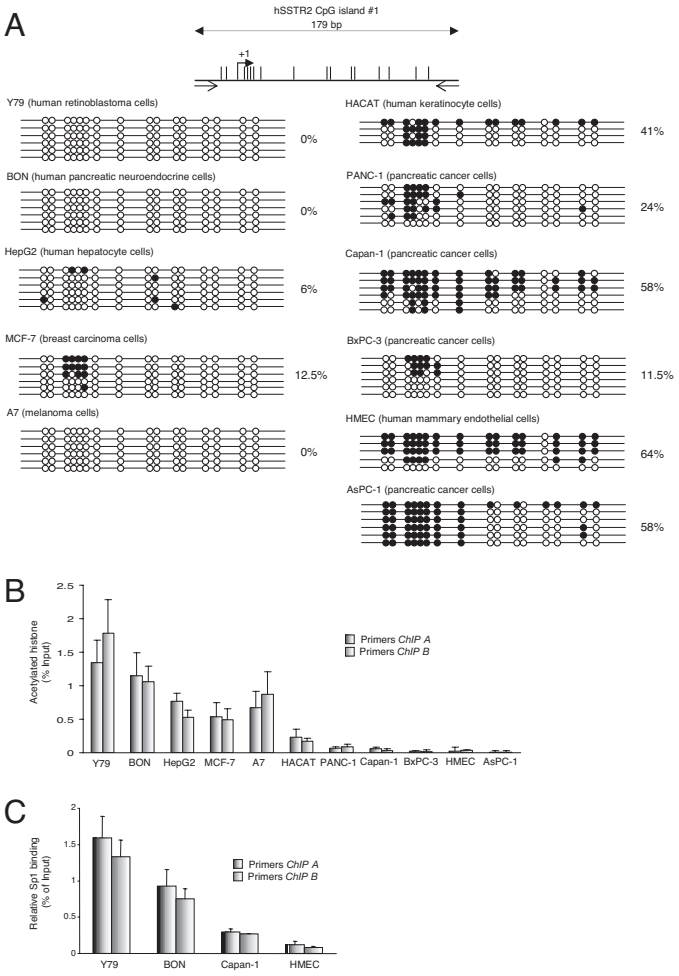

FIG. 6. High levels of DNA methylation in the hSSTR2 CpG island 1 correlate with low association with acetylated histones and interferes with Sp1 transcription factor binding A, Genomic DNA was extracted from 11 different human cell lines and subject to sodium bisulfite mapping. The CpG island 1 (179 bp) containing the hSSTR2 upstream transcription start site and containing 16 dinucleotides CpG were analyzed. Four to six clones of each cell line were sequenced. *Empty circles* represent unmethylated CpG dinucleotides; *filled circles* represent methylated CpG dinucleotides. Percentages of methylated CpG to total CpG dinucleotides are indicated on the *right of the panel*. B, The association of the upstream hSSTR2 promoter with acetylated histones in different cell lines was measured by ChIP. Immunoprecipitated DNA fragments were quantified by q-PCR using two sets of primers represented in Fig. 4A. Association with acetylated histone is represented as a percentage of input. C, The association of the upstream hSSTR2 promoter with the transcription factor Sp1 in Y79, BON, Capan-1, and HMEC cells was measured by ChIP assay. Immunoprecipitated DNA fragments by Sp1 antibody were quantified by q-PCR using two sets of primers represented in Fig. 4A. Sp1 binding is calculated as percentage of input.

level of DNA methylation in the hSSTR2 upstream promoter correlates to a low association with acetylated histones. This epigenetic status is inversely correlated to Sp1 binding and hSSTR2 mRNA expression.

DNA methylation affects the transcription from the hSSTR2 upstream promoter

We showed an inverse correlation between the percentage of methylated CpG within the upstream promoter and the level of hSSTR2 mRNA expression. By *in vitro* methylation assay, we investigated whether the methylation of the upstream promoter had a causal role on mRNA expression transcribed from this promoter. Transcriptional activity of an *in vitro* methylated-hSSTR2 upstream promoter was measured after transfection in Capan-1, PANC-1, MCF-7, BON, and Y79 cells (Fig. 7A). These cell lines display different methylation levels of the endogenous hSSTR2 upstream promoter [from 0% in BON and Y79 cells to 58% in Capan-1 cells (Fig. 6A)]. First, we verified that the cells had the transcriptional machinery (*i.e.* specific transcription factors) to allow basal transcription from a nonmethylated hSSTR2 upstream promoter (supplementary data S4). We then observed that in all the cell lines, the *in vitro* methylation led to a significant inhibition of hSSTR2 upstream promoter activity. These data demonstrated that DNA methylation can cause the silencing of the hSSTR2 upstream promoter *in vitro*.

A combined 5-aza-2-deoxycytidine (5-aza-dC)/trichostatin A (TSA) treatment increases transcription from the hSSTR2 upstream promoter in PANC-1, Capan-1, and HMEC cell lines

We observed an inverse correlation between the level of hSSTR2 mRNA expression and the methylation level of its upstream promoter. We also demonstrated that DNA methylation of the hSSTR2 upstream promoter alters its transcriptional capacity. As we studied an *in vitro* methylated and

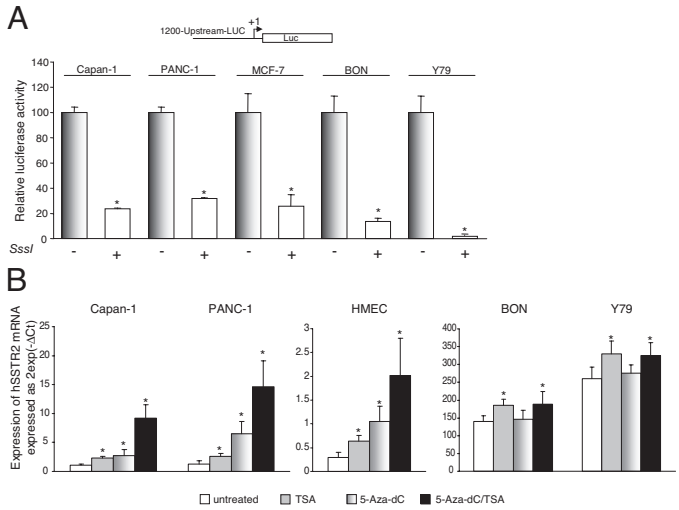

FIG. 7. DNA methylation and histone acetylation control hSSTR2 transcription from the upstream promoter. A, Transfections of an *in vitro* methylated 1200-Upstream-LUC or pGL_3 basic plasmids were performed in Capan-1, PANC-1, MCF-7, BON, and Y79 cells. After 24 h, transcriptional activity was measured and compared with transcriptional activity of the same amount of nonmethylated 1200-Upstream-LUC or pGL_3 basic plasmids. β-Galactosidase activity was used to normalize readings. Transfection and *in vitro* methylation experiments (n = 3) were performed in triplicate. B, Capan-1, PANC-1, HMEC, BON, and Y79 cells were grown in the presence of 5-aza-dC (2 μM) or TSA (150 nM) alone or in combination. Seventy-two hours after transfection, total RNAs were isolated and subject to RT. The amount of hSSTR2 transcribed from the upstream promoter was measured by q-RT-PCR. Results are expressed as 2exp(-ΔCt) using β-actin as the reference gene. Treatment and q-RT-PCR were performed in triplicates.

nonchromatinized DNA (Fig. 7A and supplementary data S4), we aimed to confirm the causal role of DNA methylation on hSSTR2 upstream promoter silencing in living cells. Capan-1, PANC-1, HMEC, BON, and Y79 cells displaying different levels of hSSTR2 mRNA expression and CpG methylation in the upstream region (Figs. 2, 5, and 6A) were grown in the presence of a potent DNA methyltransferases inhibitor, the 5-aza-dC in combination or not with a histone deacetylase inhibitor, TSA. After 72 h, the level of hSSTR2 mRNA transcribed from the upstream promoter was measured by q-RT-PCR (Fig. 7B). Whereas the treatment with TSA slightly affected the level of hSSTR2 mRNA in the cell lines tested, the treatment with the 5-aza-dC significantly increased this mRNA level in Capan-1, PANC-1, and HMEC cells. More interestingly, the cotreatment with 5-aza-dC and TSA led to a greater effect on hSSTR2 mRNA production in a synergistic manner in Capan-1, PANC-1, and HMEC cells (8.4-, 11.2-, and 6.7-fold induction, respectively). This cotreatment only slightly modified hSSTR2 mRNA level in BON and Y79 cells. The hSSTR2 mRNA increase in Capan-1, PANC-1, and HMEC cells was correlated with a reduction of the methylation level of the upstream promoter induced by the cotreatment 5-aza-dC/TSA (58 to 10, 24 to 2, and 64 to 6%, respectively) (supplementary data S5). No effect of this cotreatment on this methylation level was observed in BON and Y79 cells in which the upstream promoter is not methylated (Fig. 6A and supplementary data S5).

The increased expression of hSSTR2 mRNA after DNA methyltransferase inhibitor in three cell lines in which the hSSTR2 upstream region is methylated confirmed that DNA methylation is strongly involved in maintenance of a low level of hSSTR2 mRNA. Moreover, the synergistic effect of the treatment with the HDAC inhibitor reinforced the fact that histone acetylation participates in the silencing of hSSTR2 gene in these cell lines.

Discussion

Here we present evidence for a novel upstream promoter region in the hSSTR2 gene located approximately 4.2 kb upstream from the initially described promoter region (9, 15, 16). We find that in addition to its basal transcription activity, which is mediated by the transcription factor Sp1, the upstream promoter is controlled by two epigenetic modifications, DNA methylation and histone acetylation. We further show that the epigenetic regulation of this promoter region results in differential expression of hSSTR2 in human cell lines.

Discovery of two CpG islands located approximately 3.8 kb upstream from the transcription start site suggested the existence of an upstream promoter (Fig. 1). To facilitate the identification of an upstream promoter, we first identified human cell lines that express high levels of hSSTR2 mRNA expression. We measured by q-RT-PCR this level in 11 different human cell lines (Fig. 2). Among them we found that the retinoblastoma Y79, breast cancer MCF-7, and pancreatic neuroendocrine BON cells expressed high levels of hSSTR2 mRNA. The high level of hSSTR2 mRNA in retinoblastoma Y79 cells were in accordance with the work of Klisovic *et al.* (34) in which he showed a wide expression in human eye. Previous works also revealed expression of hSSTR2 receptor in human breast cancer (35) and MCF-7 cells (15). High level of somatostatin receptor expression is a hallmark of gastroenteropancreatic endocrine tumors (36). The high expression level observed in pancreatic neuroendocrine BON cells was therefore anticipated. In contrast, the low levels of hSSTR2 mRNA expression in human exocrine pancreatic cancer cell lines tested are in accordance with our and other previous studies that showed a reduction in hSSTR2 expression in human pancreatic cancer and most derived cell lines (10–12).

Although the existence of upstream promoters were identified for the human SSTR5 and murine SSTR2 genes (18, 19), the existence of such an upstream promoter for the human SSTR2 gene was only suggested by Kraus *et al.* (18) but not identified. The difficulty in identifying this upstream transcription start site was most probably due to the low level of expression in most cell lines. The fact that this promoter region is silenced by DNA methylation in numerous cell lines might also explain these low levels of expression. The high CG content of the novel mRNA 5′-UTR may lead to strong secondary structures that could also affect the efficiency of the RT process. All these parameters led us to perform our 5′-RACE assay including a RT step at 50 C on RNAs extracted from Y79 cells that express a high level of hSSTR2 mRNA (Fig. 3A). The presence of this upstream promoter region leads to the transcription of two different mRNA transcripts (Fig. 3B). Although the mRNA transcribed from the upstream promoter contains a longer 5′-UTR, the amino acid sequence of hSSTR2 receptor does not change. Indeed, the extended 5′-UTR region does not contain a transitional initiation ATG codon that is in frame with the open reading frame. Although the two transcripts do not change the amino acid sequence of the receptor, we cannot exclude that the longer transcripts form RNA secondary structures thereby affecting translation efficiency. This possibility will be further studied.

By bioinformatic approaches, we found high homologies between human upstream hSSTR2 sequence (~1.2 kb) and rat exon 1 upstream sequence as well as mouse exon 2 upstream sequence. Putative transcription factor binding sites highly conserved in the three species were identified (Fig. 4A). We demonstrated that the transcription factor Sp1 is strongly involved in the basal transcriptional activity hSSTR2 upstream promoter (Fig. 4, B and C) (15). Sp1 was also shown to regulate the basal activity of the upstream rat SSTR2 promoter and mouse promoter 2 (18, 19).

In Figure 5, we showed that the usage of the hSSTR2 upstream promoter depends on the cell type. We established an inverse correlation between DNA methylation levels of hSSTR2 CpG island 1 and hSSTR2 mRNA expression from the upstream promoter but also the binding of the transcription factor Sp1 (Figs. 5 and 6, A and C). Although our findings were consistent among most cell lines, we observed a similar percentage of methylated hSSTR2 CpG island (12.5 and 11.5%, respectively) (Fig. 6A) but different levels of hSSTR2 mRNA expression from the upstream promoter in two cell lines (MCF-7 and BxPC-3) (Fig. 5). These findings strongly suggest that other DNA regions within the CpG island might be differently methylated, a subject of further study. One other explanation might be that a lack of the transcription factor small mothers against decapentaplegic-4/deleted in pancreatic carcinoma-4 is responsible of the low expression in BxPC-3 cells as was previously demonstrated

(37). Different Sp1 level in these cells might also contribute to a differential regulation.

The causal role of DNA methylation in the regulation of the hSSTR2 upstream promoter was demonstrated by *in vitro* methylation assay (Fig. 7A). When *in vitro* methylated by *Sss* I enzyme, the transcriptional activity of the hSSTR2 upstream promoter is dramatically decreased, demonstrating the causal role of DNA methylation in the repression of this promoter. Furthermore, Capan-1, PANC-1, HMEC, BON, and Y79 cells were grown in the presence of 5-aza-dC or TSA alone or in combination (Fig. 7B). Whereas the treatment with TSA slightly affects hSSTR2 mRNA expression in the cell lines tested, the treatment with 5-aza-dC leads to an increase of hSSTR2 mRNA in Capan-1, PANC-1, and HMEC cells in which the upstream promoter is methylated (Fig. 6A), Moreover, the effect of 5-aza-dC on hSSTR2 mRNA expression in this hSSTR2-low-expressing cell lines is enhanced by the addition of TSA in a synergic manner. These results confirm the strong participation of the two epigenetic modifications, DNA methylation and histone acetylation, in the regulation of the hSSTR2 upstream promoter.

Although the role of promoter methylation in gene silencing is well established in cancer cells (25), there are few studies demonstrating that such mechanisms affect alternative promoter regions of genes. Archey *et al.* (38) reported the methylation status of an alternative promoter for the human transforming growth-β-3, and correlated these findings with its activity. Moreover, a causal link between alternative promoter methylation and silencing of the respective isoform has been demonstrated for transcript A of the human RAS effector homolog (39). Another study implied DNA methylation in the regulation of alternative promoters encoding stem cell surface protein AC133 (40). We propose that such an alternative promoter usage may increase diversity and flexibility in gene expression depending on the cell type. Stable changes, such as those imposed by DNA methylation, might represent a permanent mechanism for the cell to modulate hSSTR2 expression.

Recently studies have also demonstrated the contribution of the transcription factor Sp1 in the basal activity of the hSSTR2 upstream promoter. We further proposed that the binding of this transcription factor can vary, depending on the methylation level of this upstream region (Fig. 6C). They observed a transcriptional activation of this promoter by an estrogen stimulation suggesting another mechanism of regulation for hSSTR2 gene (41).

Somatostatin analog treatment is the most common treatment of endocrine tumors. This treatment is feasible because of the high expression level on the somatostatin receptors on these tumors through which somatostatin stable analogs can exert their antisecretory and antiproliferative effects. The perspective to use demethylating agents (decitabine) and/or histone deacetylase inhibitors (TSA) in combination with somatostatin analog treatment could be promising. A combined treatment could bring about greater efficacy in the treatment of these endocrine tumors. More interestingly, treatment of low hSSTR2-expressing tumors (*i.e.* pancreatic adenocarcinomas) with demethylating agents and/or deacetylase inhibitors could aid in restoring sufficient expression levels of hSSTR2 that might permit a significant effect of a somatostatin analog treatment. This therapeutic benefit of a combined treatment is supported by the recent study in which Gahr *et al.* (42) showed that the combination of the histone-deacetylase inhibitor TSA and gemcitabine induces inhibition of proliferation and increased apoptosis in pancreatic carcinoma cells. The DNA methylation inhibitors 5-azacytidine, 5-aza-dC (decitabine) and 5,6-dihydro-5-azacytidine have been used as cancer chemotherapeutic agents in clinical trials on various neoplasms. Unfortunately, for solid tumors little clinical efficacy is observed with no disease stabilization, and these are accompanied by many toxic effects (43). The best outcomes of treatment with 5-azacytidine or 5-aza-dC were seen for patients with refractory or relapsed acute leukemia (44). Therefore, the perspective of a combined treatment of DNA methylation inhibitors and somatostatin analogs will depend on the development of new DNA methylation inhibitors that will display less toxic effects on solids tumors. However, a new perspective came out from our recent research (45). Indeed, 5-azacytidine is a prodrug that is activated by phosphorylation by deoxycytidine kinase (46). We rendered gemcitabine more efficient in the treatment of pancreatic tumors by expressing a fusion protein combining deoxycytidine kinase and the uridine monophosphate kinase by gene therapy. Overexpression of a 5-azacytidine-activating enzyme may render 5-azacytidine more efficient at a lower concentration generating less toxic effects. The perspective of a combined treatment of DNA methylation inhibitors with somatostatin analogs can be envisaged.

Acknowledgments

We thank Dr. S. Shaak and Dr. H. Paris for providing us MCF-7 cells and pCMV-Sp1, -Sp3, and -Sp4 vectors; H. Laklaï for HMEC cells, S. Laval [Institut National de Santé et Recherche Médicale (INSERM) 858, Toulouse, France] for HACAT cells; and Dr. J. F. Bruno (Stony Brook University, Stony Brook, NY) for pBluescript II hsst2p plasmid. We also acknowledge N. Saint Laurent (INSERM 858, Toulouse, France) for melanoma A7 cells and technical assistance; Dr. D. Arvanitis (Center of Developmental Biology, Toulouse) for critical reading of the manuscript; and Dr. C. Bureau (INSERM 858, Toulouse, France) for his help in statistical analysis.

Received November 7, 2007. Accepted February 27, 2008.

Address all correspondence and requests for reprints to: Louis Buscail, M.D., Ph.D., Institut National de Santé et Recherche Médicale Unité 858, I2MR Institut de Médecine Moléculaire de Rangueil, Département Cancers Epithéliaux, Angiogénèse, et Signalisation 1, avenue Jean Poulhès, BP 84225, 31432 Toulouse Cedex 4, France. E-mail: louis.buscail@toulouse.inserm.fr.

This work was supported by a fellowship of the Institut National du Cancer (Inca-France (to J.T.) and grants from the Cancéropôle Grand Sud-Ouest, the Région Midi-Pyrénées, and the Association pour la Recherche contre le Cancer. H.L. was supported by a fellowship from the European Economic Community.

Disclosure Statement: The authors have nothing to disclose.

References

1. **Guillermet-Guibert J, Lahlou H, Cordelier P, Bousquet C, Pyronnet S, Susini C** 2005 Physiology of somatostatin receptors. J Endocrinol Invest 28:5–9
2. **Gillies G** 1997 Somatostatin: the neuroendocrine story. Trends Pharmacol Sci 18:87–95
3. **Susini C, Buscail L** 2006 Rationale for the use of somatostatin analogs as antitumor agents. Ann Oncol 17:1733–1742
4. **Kvols LK, Woltering EA** 2006 Role of somatostatin analogs in the clinical management of non-neuroendocrine solid tumors. Anticancer Drugs 17:601–608
5. **Patel YC, Greenwood MT, Panetta R, Demchyshyn L, Niznik H, Srikant CB** 1995 The somatostatin receptor family. Life Sci 57:1249–1265
6. **Lopez F, Esteve JP, Buscail L, Delesque N, Saint-Laurent N, Vaysse N, Susini C** 1996 Molecular mechanisms of antiproliferative effect of somatostatin: involvement of a tyrosine phosphatase. Metabolism 45:14–16
7. **Buscail L, Esteve JP, Saint-Laurent N, Bertrand V, Reisine T, O'Carroll AM,**

Bell GI, Schally AV, Vaysse N, Susini C 1995 Inhibition of cell proliferation by the somatostatin analogue RC-160 is mediated by somatostatin receptor subtypes SSTR2 and SSTR5 through different mechanisms. Proc Natl Acad Sci USA 92:1580–1584

8. **Guillermet-Guibert J, Saint-Laurent N, Davenne L, Rochaix P, Cuvillier O, Culler MD, Pradayrol L, Buscail L, Susini C, Bousquet C** 2007 Novel synergistic mechanism for sst2 somatostatin and TNFα receptors to induce apoptosis: crosstalk between NF-κB and JNK pathways. Cell Death Differ 14:197–208
9. **Greenwood MT, Robertson LA, Patel YC** 1995 Cloning of the gene encoding human somatostatin receptor 2: sequence analysis of the 5′-flanking promoter region. Gene 159:291–292
10. **Li M, Li W, Kim HJ, Yao Q, Chen C, Fisher WE** 2004 Characterization of somatostatin receptor expression in human pancreatic cancer using real-time RT-PCR. J Surg Res 119:130–137
11. **Buscail L, Saint-Laurent N, Chastre E, Vaillant JC, Gespach C, Capella G, Kalthoff H, Lluis F, Vaysse N, Susini C** 1996 Loss of sst2 somatostatin receptor gene expression in human pancreatic and colorectal cancer. Cancer Res 56: 1823–1827
12. **Fisher WE, Wu Y, Amaya F, Berger DH** 2002 Somatostatin receptor subtype 2 gene therapy inhibits pancreatic cancer *in vitro*. J Surg Res 105:58–64
13. **Reubi JC, Horisberger U, Essed CE, Jeekel J, Klijn JG, Lamberts SW** 1988 Absence of somatostatin receptors in human exocrine pancreatic adenocarcinomas. Gastroenterology 95:760–763
14. **Petersenn S, Rasch AC, Presch S, Beil FU, Schulte HM** 1999 Genomic structure and transcriptional regulation of the human somatostatin receptor type 2. Mol Cell Endocrinol 157:75–85
15. **Pscherer A, Dorflinger U, Kirfel J, Gawlas K, Ruschoff J, Buettner R, Schule R** 1996 The helix-loop-helix transcription factor SEF-2 regulates the activity of a novel initiator element in the promoter of the human somatostatin receptor II gene. EMBO J 15:6680–6690
16. **Xu Y, Berelowitz M, Bruno JF** 1998 Characterization of the promoter region of the human somatostatin receptor subtype 2 gene and localization of sequences required for estrogen-responsiveness. Mol Cell Endocrinol 139:71–77
17. **Patel YC, Greenwood M, Kent G, Panetta R, Srikant CB** 1993 Multiple gene transcripts of the somatostatin receptor SSTR2: tissue selective distribution and cAMP regulation. Biochem Biophys Res Commun 192:288–294
18. **Kraus J, Woltje M, Schonwetter N, Hollt V** 1998 Alternative promoter usage and tissue specific expression of the mouse somatostatin receptor 2 gene. FEBS Lett 428:165–170
19. **Petersenn S, Rasch AC, Bohnke C, Schulte HM** 2002 Identification of an upstream pituitary-active promoter of human somatostatin receptor subtype 5. Endocrinology 143:2626–2634
20. **Gardiner-Garden M, Frommer M** 1987 CpG islands in vertebrate genomes. J Mol Biol 196:261–282
21. **Bestor TH** 2000 The DNA methyltransferases of mammals. Hum Mol Genet 9:2395–2402
22. **Bird AP** 1980 DNA methylation and the frequency of CpG in animal DNA. Nucleic Acids Res 8:1499–1504
23. **Riggs AD, Pfeifer GP** 1992 X-chromosome inactivation and cell memory. Trends Genet 8:169–174
24. **Razin A, Cedar H** 1994 DNA methylation and genomic imprinting. Cell 77:473–476
25. **Bird AP** 1996 The relationship of DNA methylation to cancer. Cancer Surv 28:87–101
26. **Nan X, Ng HH, Johnson CA, Laherty CD, Turner BM, Eisenman RN, Bird A** 1998 Transcriptional repression by the methyl-CpG-binding protein MeCP2 involves a histone deacetylase complex. Nature 393:386–389
27. **Li L, He S, Sun JM, Davie JR** 2004 Gene regulation by Sp1 and Sp3. Biochem Cell Biol 82:460–471
28. **Zhu WG, Srinivasan K, Dai Z, Duan W, Druhan LJ, Ding H, Yee L, Villalona-Calero MA, Plass C, Otterson GA** 2003 Methylation of adjacent CpG sites affects Sp1/Sp3 binding and activity in the p21(Cip1) promoter. Mol Cell Biol 23:4056–4065
29. **Corpet F** 1988 Multiple sequence alignment with hierarchical clustering. Nucleic Acids Res 16:10881–10890
30. **Vezzosi D, Bouisson M, Escourrou G, Laurell H, Selves J, Seguin P, Pradayrol L, Caron P, Buscail L** 2006 Clinical utility of telomerase for the diagnosis of malignant well-differentiated endocrine tumours. Clin Endocrinol (Oxf) 64:63–67
31. **Torrisani J, Unterberger A, Tendulkar SR, Shikimi K, Szyf M** 2007 AUF1 cell cycle variations define genomic DNA methylation by regulation of DNMT1 mRNA stability. Mol Cell Biol 27:395–410
32. **Ogbourne S, Antalis TM** 1998 Transcriptional control and the role of silencers in transcriptional regulation in eukaryotes. Biochem J 331(Pt 1):1–14
33. **Kimura N, Tomizawa S, Arai KN, Osamura RY, Kimura N** 2001 Characterization of 5′-flanking region of rat somatostatin receptor sst2 gene: transcriptional regulatory elements and activation by Pitx1 and estrogen. Endocrinology 142:1427–1441
34. **Klisovic DD, O'Dorisio MS, Katz SE, Sall JW, Balster D, O'Dorisio TM, Craig E, Lubow M** 2001 Somatostatin receptor gene expression in human ocular tissues: RT-PCR and immunohistochemical study. Invest Ophthalmol Vis Sci 42:2193–2201
35. **Orlando C, Raggi CC, Bianchi S, Distante V, Simi L, Vezzosi V, Gelmini S, Pinzani P, Smith MC, Buonamano A, Lazzeri E, Pazzagli M, Cataliotti L, Maggi M, Serio M** 2004 Measurement of somatostatin receptor subtype 2 mRNA in breast cancer and corresponding normal tissue. Endocr Relat Cancer 11:323–332
36. **de Herder WW, Hofland LJ, van der Lely AJ, Lamberts SW** 2003 Somatostatin receptors in gastroentero-pancreatic neuroendocrine tumours. Endocr Relat Cancer 10:451–458
37. **Puente E, Saint-Laurent N, Torrisani J, Furet C, Schally AV, Vaysse N, Buscail L, Susini C** 2001 Transcriptional activation of mouse sst2 somatostatin receptor promoter by transforming growth factor-β. Involvement of Smad4. J Biol Chem 276:13461–13468
38. **Archey WB, Sweet MP, Alig GC, Arrick BA** 1999 Methylation of CpGs as a determinant of transcriptional activation at alternative promoters for transforming growth factor-β3. Cancer Res 59:2292–2296
39. **Dammann R, Li C, Yoon JH, Chin PL, Bates S, Pfeifer GP** 2000 Epigenetic inactivation of a RAS association domain family protein from the lung tumour suppressor locus 3p21.3. Nat Genet 25:315–319
40. **Shmelkov SV, Jun L, St Clair R, McGarrigle D, Derderian CA, Usenko JK, Costa C, Zhang F, Guo X, Rafii S** 2004 Alternative promoters regulate transcription of the gene that encodes stem cell surface protein AC133. Blood 103:2055–2061
41. **Kimura N, Takamatsu N, Yaoita Y, Osamura RY, Kimura N** 2008 Identification of transcriptional regulatory elements in the human somatostatin receptor sst2 promoter and regions including estrogen response element half-site for estrogen activation. J Mol Endocrinol 40:75–91
42. **Gahr S, Ocker M, Ganslmayer M, Zopf S, Okamoto K, Hartl A, Leitner S, Hahn EG, Herold C** 2007 The combination of the histone-deacetylase inhibitor trichostatin A and gemcitabine induces inhibition of proliferation and increased apoptosis in pancreatic carcinoma cells. Int J Oncol 31:567–576
43. **Abele R, Clavel M, Dodion P, Bruntsch U, Gundersen S, Smyth J, Renard J, van Glabbeke M, Pinedo HM** 1987 The EORTC Early Clinical Trials Cooperative Group experience with 5-aza-2′-deoxycytidine (NSC 127716) in patients with colo-rectal, head and neck, renal carcinomas and malignant melanomas. Eur J Cancer Clin Oncol 23:1921–1924
44. **Santini V, Kantarjian HM, Issa JP** 2001 Changes in DNA methylation in neoplasia: pathophysiology and therapeutic implications. Ann Intern Med 134:573–586
45. **Vernejoul F, Ghenassia L, Souque A, Lulka H, Drocourt D, Cordelier P, Pradayrol L, Pyronnet S, Buscail L, Tiraby G** 2006 Gene therapy based on gemcitabine chemosensitization suppresses pancreatic tumor growth. Mol Ther 14:758–767
46. **Momparler RL, Derse D** 1979 Kinetics of phosphorylation of 5-aza-2′-deoxycytidine by deoxycytidine kinase. Biochem Pharmacol 28:1443–1444

Endocrinology **is published monthly by The Endocrine Society (http://www.endo-society.org), the foremost professional society serving the endocrine community.**